17th Brazilian Congress of Thermal Sciences and Engineering
November 25th-28th, 2018, Águas de Lindóia, SP, Brazil

# ENCIT-2018-0125
# ANALYSIS OF LAMINAR FORCED CONVECTION ASYMMETRIC OF NON-NEWTONIAN FLUID IN THE THERMAL ENTRANCE REGION OF A CHANNEL OF PARALLEL PLATES

**Dhiego Luiz de Andrade Veloso**
**Carlos Antônio Cabral dos Santos**
UFPB-PPGEM, Cidade Universitária - João Pessoa - PB - Brasil - CEP: 58051-900
dhiego_vel@hotmail.com
carloscabralsantos@yahoo.com.br

***Abstract.*** *The present work aims at analyzing the heat transfer in a flow inside a channel of parallel flat plates. It is considered that flat plates to have distincts thermophysical properties and that they are in contact with thermal reservoirs with different temperatures, in which guarantees an asymmetry in the problem studied. The flowing fluid is considered non-Newtonian of power law type. The Classical Integral Transformation Technique (CITT) was used to solve the energy equation. The temperature field and the local Nusselt numbers in the upper and lower plates are evaluated for several values of the power law index and the Biot number. The obtained results were confronted with existing ones in the open literature in order to validate the presented model.*

***Keywords:*** *flat plates, asymmetry, CITT, temperature field, Nusselt.*

## 1. INTRODUCTION

With the great technological advance of modernity it becomes providential a thorough knowledge about the real processes of heat transfer, as well arise a need to analyze them quantitatively. Such an advance brings forth, increasingly, extremely complex engineering problems, requiring precise solutions in a short period of time that provide the optimization of the resources employed and that satisfies the market need. In this context, numerical methods have been gaining strength and achieving good approximations to the desired solutions. With the advent of high-tech computers, these problems, which in the great majority do not present analytical solution, can be treated by numerical approximation methods which are quite useful in engineering applications (Diniz, 2005). Due to the increasing need for accurate solutions in a short period of time, the numerical approximation techniques have gained space over the experimentation and the classical analytical methods. This occurs because the experimentation almost always very time consuming and the costs of acquiring and gauging of equipment are enormous for each new situation, and classical analytical methods have certain limitations (Veronese *et al.*, 2012).

In particular, problems of diffusion of heat and mass, area of study of great interest of the engineering by attending to several practical situations, the CITT presents itself as a consecrated methodology having been successfully used in several classes of heat transfer and fluid mechanics problems, as can be seen in (Mikhailov e Özisik, 1984).

The heat transfer in laminar forced convection of Newtonian or non-Newtonian fluids in the thermal entrance region of circular and rectangular ducts has been studied both analytically and numerically for the various boundary conditions (Norris and Streid, 1940; Shah, 1975; Johnston, 1994; Chalhub, 2011; Veronese *et al.*, 2012 and Assad *et al.*, 2018). A fairly comprehensive review of the literature can be found in the works of (Kakaç *et. al*, 2014; Shah and London, 2014 and SANTOS *et al.*,2001).

The problem to be studied is a developed flow of non-Newtonian fluid of power law type, inside a channel of parallel flat plates, subject to the contour conditions of the 3$^{rd}$ type (Robin's condition, due to heat exchange with the environment), as shown in Fig. 1. It can be verify that the flat plates have different thermal conductivities and distinct heat transfer coefficients, besides observing that they are in thermal contact with environments that have different temperatures. In the specialized literature, usually the reference system is placed in the center of the channel taking into account the condition of symmetry in the flow. Due to the asymmetry imposed by the considerations adopted, in the present work we will take the reference in the wall corresponding to the lower plate, which allows us to analyze the problem from the viewpoint of asymmetry, that is, different contour conditions for upper and lower plates.

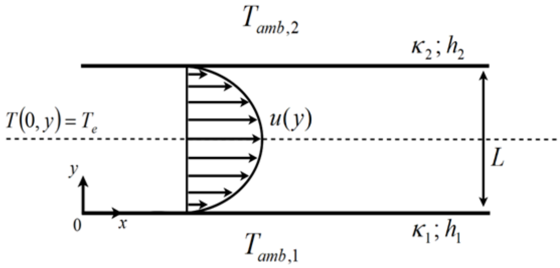


Figure 1. Problem illustration

The non-Newtonian fluids have varying viscosities in response to the stress applied to it, have an intrinsic nonlinearity. As examples it can be cite biological fluids and pharmaceuticals, petroleum, detergent, soap, plastics, among others. The present work observes the influence of rheology of the fluid on the development of the temperature Field, in addition to observing the influence of the Biot number about the local Nusselt numbers of the upper and lower plates.

## 2. MATHEMATICAL MODELING

For the mathematical modeling of the proposed physical problem, the following considerations were made:

- Laminar flow, in steady state;
- Incompressible fluid;
- The thermophysical properties of the fluid and the plates are considered constant;
- The speed profile is fully developed at the thermal input;
- The effects of viscous dissipation will not be considered;
- Impermeability and non-slip on walls;
- Neglecting body forces;
- No internal power generation;
- Uniform pressure gradient in the axial direction;
- Neglecting the axial diffusion of the fluid;
- The length of the channel is much larger than its height.

It is desired to determine the temperature distribution of the fluid. Taking into account the mentioned heat transfer problem, the mathematical modeling for a fully developed flow, shown in Fig. 1, can be written as follows:

**Energy equation**

$$\rho C_P u(y)\frac{\partial T(x,y)}{\partial x} = \kappa_f \frac{\partial^2 T(x,y)}{\partial y^2} \quad ; \quad x \geq 0 \text{ and } 0 \leq y \leq L \tag{1}$$

where $\rho$, $C_P$ and $\kappa_f$ represent, respectively, the specific mass, the specific heat at constant pressure and the thermal conductivity of the fluid. The velocity field, proposed in the present work, for the fully developed flow mentioned, solving the Navier-Stokes equations and considering the non-slip on the walls, as well as the reference system adopted, it is given by:

$$u(y) = \frac{2n+1}{n+1}u_m\left\{1-\left[1-2\left(\frac{y}{L}\right)\right]^{\frac{n+1}{n}}\right\} \quad ; \quad 0 \leq y \leq L/2 \tag{2}$$

$$u(y) = \frac{2n+1}{n+1}u_m\left\{1-\left[2\left(\frac{y}{L}\right)-1\right]^{\frac{n+1}{n}}\right\} \quad ; \quad L/2 \leq y \leq L \tag{3}$$

where $u_m$ corresponds to the average flow velocity and $n$ represents the power law index. If $n$=1, the fluid is Newtonian, if $n$>1, the fluid is dilatant and if $n$<1, the fluid is pseudoplastic.

**Contour Conditions**

$$-\kappa_1 \frac{\partial T(x,y)}{\partial y} = h_1\left[T(x,y) - T_{amb,1}\right] \; ; \; y = 0 \text{ and } x > 0 \tag{4}$$

$$-\kappa_2 \frac{\partial T(x,y)}{\partial y} = h_2\left[T(x,y) - T_{amb,2}\right] \; ; \; y = L \text{ and } x > 0 \tag{5}$$

**Inlet condition**

$$T(x,y) = T_e \; ; \; x = 0 \text{ and } 0 \le y \le L \tag{6}$$

## 2.1 Dimensionless Form

For the analysis of the problem were defined the following dimensionless parameters, given by equations (7a-j), with the objective of solving not only a particular problem, but a class of problems that are defined by the same proposed model.

$$X = \frac{\alpha.x}{L^2.u_m} \qquad \varsigma = \frac{y}{L} \qquad u(\varsigma) = \frac{u(y)}{u_m} \qquad Bi_1 = \frac{h_1.L}{\kappa_1} \qquad Bi_2 = \frac{h_2.L}{\kappa_2} \qquad \Pr = \frac{\upsilon}{\alpha} \tag{7a-f}$$

$$\Theta(X,\varsigma) = \frac{T(x,y) - T_{amb,1}}{T_e - T_{amb,1}} \quad \Theta_2 = \frac{T_{amb,2} - T_{amb,1}}{T_e - T_{amb,1}} \quad \mathrm{Re}_h = \frac{D_h.u_m}{\upsilon} \quad P_e = \mathrm{Re}_h.\Pr = \frac{D_h u_m}{\alpha} \tag{7g-j}$$

where $\nu$ is the kinematic viscosity, $\alpha$ is the thermal diffusivity of the fluid, $\kappa_1$ is the thermal conductivity of the lower plate, $\kappa_2$ is the thermal conductivity of the upper plate, $L$ is the distance between the plates, $D_h = 2.L$ is the hydraulic diameter, $h_1$ corresponds to the heat transfer coefficient of the lower plate, $h_2$ is the heat transfer coefficient of the upper plate and $Pr$ , $Re_h$ and $Pe$ are, respectively, the numbers of Prandtl, Reynolds and Peclet.

Applying the dimensionless parameters in equations (1), (2), (3), (4) and (5), we find the energy equation, the boundary conditions and the inlet condition in the dimensionless form:

**Energy equation dimensionless**

$$u(\varsigma)\frac{\partial \Theta(X,\varsigma)}{\partial X} = \frac{\partial^2 \Theta(X,\varsigma)}{\partial \varsigma^2} \; ; \; X > 0 \text{ and } 0 \le \varsigma \le 1 \tag{8}$$

**Boundary conditions dimensionless**

$$\frac{\partial \Theta(X,\varsigma)}{\partial \varsigma} + Bi_1.\Theta(X,\varsigma) = 0 \; ; \quad \varsigma = 0 \text{ and } X > 0 \tag{9}$$

$$\frac{\partial \Theta(X,\varsigma)}{\partial \varsigma} + Bi_2.\Theta(X,\varsigma) = Bi_2.\Theta_2 \; ; \quad \varsigma = 1 \text{ and } X > 0 \tag{10}$$

**Inlet condition dimensionless**

$$\Theta(X,\varsigma) = 1, \qquad 0 \le \varsigma \le 1, \qquad X = 0 \tag{11}$$

Since the problem has a non-homogeneous boundary condition in the $\varsigma$ direction, given by eq. (10), a mathematical filter will be used for CITT be applied properly, as well as to improve computational performance. The proposed filter be of the form:

$$\Theta(X,\varsigma)=\Theta^*(X,\varsigma)+\Theta_F(\varsigma) \tag{12}$$

The introduced mathematical filter is given by:

$$\Theta_F(\varsigma)=\frac{Bi_2\Theta_2}{Bi_2-Bi_1Bi_2-Bi_1}\left[1-Bi_1.\varsigma\right] \tag{13}$$

The CITT will be applied in $\Theta^*(X,\varsigma)$, where it will be possible to obtain its solution. Through this solution, we will use equations (13) and (12) to find the general solution of the proposed physical problem. Following the CITT methodology, appropriate auxiliary problems must be defined, as well as the development of a transformed-inverse pair.

### 2.2 Auxiliar eigenvalue problem in the radial direction

The auxiliary problem for the temperature field falls on the typical Sturm-Liouville problem. The auxiliary eigenvalue problem for the determination of the temperature field is written as follows:

$$\frac{d^2\Psi_i(\varsigma)}{d\varsigma^2}+\mu_i^2u(\varsigma)\Psi_i(\varsigma)=0, \qquad 0\le\varsigma\le 1 \tag{14}$$

$$\frac{d\Psi_i(\varsigma)}{d\varsigma}+Bi_1.\Psi_i(\varsigma)=0 \quad ; \quad \varsigma=0 \tag{15}$$

$$\frac{d\Psi_i(\varsigma)}{d\varsigma}+Bi_2.\Psi_i(\varsigma)=0 \quad ; \quad \varsigma=1 \tag{16}$$

In the present work the integral transform method is used to determine the eigenvalues ($\mu_i$), the eigenfunctions, $\Psi_i(\varsigma)$, and the norms ($N_i$), as described by (Cotta, 1993). The integral transform method was implemented in the computational code in the Fortran INTEL platform to solve the associated eigenvalue problem.

### 2.3 Integral transformation of the temperature field

Following the methodology of use of CITT, we will define a transformed-inverse pair with the purpose of reducing the original problem, that it is a partial differential equation, in an infinite and coupled system of ordinary differential equations. In a second moment, the inverse formula can be used to obtain the solution of the original problem (Cotta, 1993 and 1998). The integral transformed pair defined for this problem is given by:

$$\overline{\Theta}_i(X)=\frac{1}{N_i^{1/2}}\int_0^1 u(\varsigma).\Psi_i(\varsigma)\Theta^*(X,\varsigma)d\varsigma, \qquad \textit{Transformed} \tag{17}$$

$$\Theta^*(X,\varsigma)=\sum_{i=0}^{\infty}\frac{\Psi_i(\varsigma)\overline{\Theta}(X)}{N_i^{1/2}}, \qquad \textit{Inverse} \tag{18}$$

Analytically treating equation (8) by means of integral operators, with the aid of the auxiliary problem and the transformed-inverse pair, we can transform this partial differential equation into a system of ordinary differential equations given by:

$$\frac{d\overline{\Theta}_i(X)}{dX}+\mu_i^2\overline{\Theta}_i(X)=0 \tag{19}$$

whose general solution is classical, given by:

$$\overline{\Theta}_i(X)=\overline{\Theta}_i(0)e^{-\mu_i^2X} \quad \text{where:} \quad \overline{\Theta}_i(0)=\frac{1}{N_i^{1/2}}\int_0^1 u(\varsigma).\Psi_i(\varsigma)d\varsigma=\bar{f}_i \tag{20-21}$$

From this solution, we can use the inverse formula, given by Eq. (18), to find the general solution of the proposed physical problem.

The average temperature dimensionless can be calculated by the expression:

$$\Theta(X)_{av.} = \frac{\int_0^1 u(\varsigma).\Theta(X,\varsigma)d\varsigma}{\int_0^1 u(\varsigma)d\varsigma} \tag{22}$$

Considering $Nu_1(X)$ the Local Nusselt number on the lower plate, and $Nu_2(X)$ the Local Nusselt number on the upper plate, we have to:

$$Nu_1(X) = -\frac{2}{\Theta(X,0)-\Theta(X)_{av.}} \left.\frac{d\Theta(X,\varsigma)}{d\varsigma}\right|_{\varsigma=0} \tag{23}$$

$$Nu_2(X) = -\frac{2}{\Theta(X)_{av.}-\Theta(X,1)} \left.\frac{d\Theta(X,\varsigma)}{d\varsigma}\right|_{\varsigma=1} \tag{24}$$

## 3. RESULTS

### 3.1 Validation of results (Symmetric case)

For the purposes of *benchmarking* the results of the present study were confronted with results found in the specialized literature, particularly in Shah(1975), Chalhub (2011) and Assad *et al.(*2018), showing the robustness and effectiveness of CITT in solving of proposed physical problem. The comparison is made for the classical case, where the symmetry condition is taken into account and the reference system is puts in the center of the channel. In Table (1) compares the average temperature dimensionless and the local Nusselt number for the symmetric case ($Bi_1=Bi_2$ *e* $\theta_2=0$) where the fluid is considered Newtonian (*n*=1) and the temperature is specified on the walls.

In Table (2) compares the local Nusselt number for non-Newtonian fluids with different power law index and a symmetric contour condition of the 1st type, where it can be verified a good agreement with the results presented here.

**Table 1. Comparison of the average temperature dimensionless and the local Nusselt number for a Newtonian fluid with prescribed temperature in the walls**

| $X^* = 4\frac{\alpha.x}{L^2.u_m}$ | Average Temperature Dimensionless | | | Local Nusselt Number | | | |
|---|---|---|---|---|---|---|---|
| | Shah (1975) | Assad *et al.* (2018) | Present Work | Shah (1975) | Assad *et al.* (2018) | Present Work $Nu_1(X)$ | Present Work $Nu_2(X)$ |
| 0.016 | 0.92774 | 0.92774 | 0.92774 | 12.822 | 12.82173 | 12.82174 | 12.82174 |
| 0.032 | 0.88604 | 0.88604 | 0.88604 | 10.545 | 10.54481 | 10.54481 | 10.54481 |
| 0.048 | 0.85137 | 0.85137 | 0.85138 | 9.5132 | 9.51325 | 9.51325 | 9.51325 |
| 0.064 | 0.82065 | 0.82065 | 0.82065 | 8.9100 | 8.90998 | 8.90999 | 8.90999 |
| 0.080 | 0.79258 | 0.79258 | 0.79258 | 8.5166 | 8.51664 | 8.51664 | 8.51664 |
| 0.096 | 0.76648 | 0.76648 | 0.76648 | 8.2456 | 8.24558 | 8.24558 | 8.24558 |
| 0.112 | 0.74191 | 0.74191 | 0.74191 | 8.0532 | 8.05322 | 8.05323 | 8.05323 |
| 0.128 | 0.71860 | 0.71860 | 0.71860 | 7.9146 | 7.91461 | 7.91461 | 7.91461 |
| 0.144 | 0.69636 | 0.69636 | 0.69636 | 7.8139 | 7.81392 | 7.81392 | 7.81392 |
| 0.160 | 0.67503 | 0.67503 | 0.67503 | 7.7405 | 7.74050 | 7.74050 | 7.74050 |
| 1.600 | 0.04459 | 0.04459 | 0.04459 | 7.5407 | 7.54070 | 7.54070 | 7.54070 |

**Table 2. Comparison of the local Nusselt number for non-Newtonian fluids with prescribed temperature in the walls**

| $X^*$ / $n$ | $X^* = 0.002$ | | | | | $X^* = 0.02$ | | | | |
|---|---|---|---|---|---|---|---|---|---|---|
| | Chalhub (2011) **FVM** | Chalhub (2011) **GITT** | Assad *et al.* (2018) | Present Work $Nu_1(X)$ | Present Work $Nu_2(X)$ | Chalhub (2011) **FVM** | Chalhub (2011) **GITT** | Assad *et al.* (2018) | Present Work $Nu_1(X)$ | Present Work $Nu_2(X)$ |
| *n*=0.5 | 26.8448 | 26.8453 | 26.8448 | 26.8451 | 26.8451 | 12.9082 | 12.9082 | 12.9082 | 12.9082 | 12.9082 |
| *n*=1.0 | 24.6882 | 24.6885 | 24.6882 | 24.6884 | 24.6884 | 12.0145 | 12.0145 | 12.0145 | 12.0145 | 12.0145 |
| *n*=2.0 | 23.3941 | 23.3943 | 23.3941 | 23.3942 | 23.3942 | 11.4618 | 11.4618 | 11.4618 | 11.4618 | 11.4618 |
| *n*=10 | 22.2101 | 22.2103 | 22.2101 | 22.2102 | 22.2102 | 10.9469 | 10.9469 | 10.9469 | 10.9469 | 10.9469 |
| *n*=50 | 21.9535 | 21.9537 | 21.9535 | 21.9536 | 21.9536 | 10.8343 | 10.8343 | 10.8343 | 10.8343 | 10.8343 |

| $X^*$ / $n$ | $X^* = 0.2$ | | | | | $X^* = 2$ | | | | |
|---|---|---|---|---|---|---|---|---|---|---|
| | Chalhub (2011) **FVM** | Chalhub (2011) **GITT** | Assad *et al.* (2018) | Present Work $Nu_1(X)$ | Present Work $Nu_2(X)$ | Chalhub (2011) **FVM** | Chalhub (2011) **GITT** | Assad *et al.* (2018) | Present Work $Nu_1(X)$ | Present Work $Nu_2(X)$ |
| *n*=0.5 | 8.04903 | 8.04903 | 8.04903 | 8.04903 | 8.04903 | 7.93976 | 7.93976 | 7.93976 | 7.93976 | 7.93976 |
| *n*=1.0 | 7.63215 | 7.63215 | 7.63215 | 7.63215 | 7.63215 | 7.54070 | 7.54070 | 7.54070 | 7.54070 | 7.54070 |
| *n*=2.0 | 7.35890 | 7.35890 | 7.35890 | 7.35890 | 7.35890 | 7.27790 | 7.27790 | 7.27790 | 7.27790 | 7.27790 |
| *n*=10 | 7.09586 | 7.09586 | 7.09586 | 7.09586 | 7.09586 | 7.02415 | 7.02415 | 7.02415 | 7.02415 | 7.02415 |
| *n*=50 | 7.03742 | 7.03742 | 7.03742 | 7.03742 | 7.03742 | 6.96769 | 6.96769 | 6.96769 | 6.96769 | 6.96769 |

Now we will analyze the development of the temperature field, explaining the thermal input length for each case analyzed. In the present work we define the thermal input length as the largest dimensionless length necessary for the fluid to reach its final temperature with a margin of 10% relative difference. The Figures (2-4) show the development of the thermal field for the symmetrical flow of a non-Newtonian fluid with constant temperature in the walls. Three cases were analyzed for the power law index (*n*= 0,25; 1 e 4), which were also studied by Assad *et al.*(2018). A good agreement can be perceived, as can be seen in table 3.

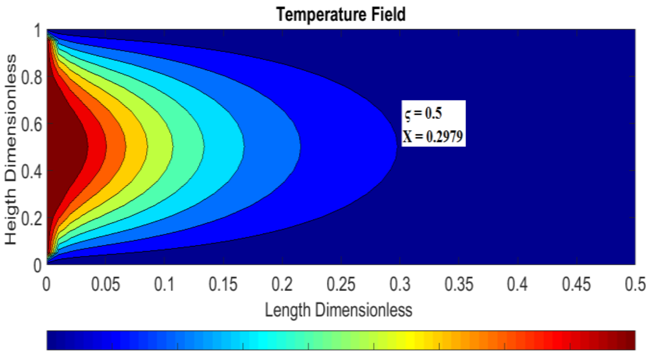


**Figure 2.** Thermal field for *n*=0.25, showing its thermal development length

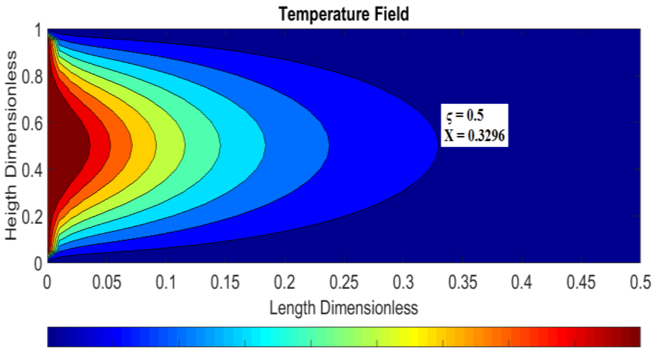


**Figure 3.** Thermal field for *n*=1, showing its thermal development length

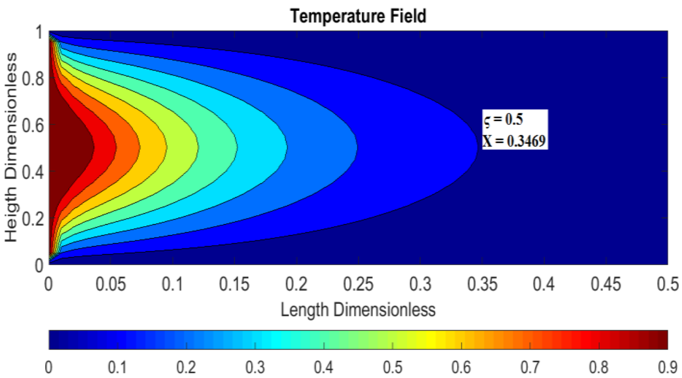


**Figure 4.** Thermal field for *n*=4, showing its thermal development length

**Table 3. Comparison of the thermal development length for different power law index**

| | ***n*=0.25** | ***n*=1** | ***n*=4** |
|---|---|---|---|
| Assad *et al.*(2018) | $L_{td,t} = 0.2965$ | $L_{td,t} = 0.3295$ | $L_{td,t} = 0.3465$ |
| Present Work | $L_{td,t} = 0.2979$ | $L_{td,t} = 0.3296$ | $L_{td,t} = 0.3469$ |

### 3.2 Obtained Results (Asymmetric Case)

In this section we will analyze the case where the flow is asymmetric ($Bi_1 \neq Bi_2$), evaluating the influence of the asymmetry consideration on the development of the temperature field and on the Local Nusselt numbers in the lower and upper plates. For all the graphs and tables contained in this paper, 200 eigenvalues and 200 corresponding eigenfunctions were used in the auxiliary problem. For all the cases analyzed below it is considered that $Bi_1 \to \infty$, varying only the values of the Biot number in the upper plate ($Bi_2$), the values of the power law index ($n$) and the values for the relative temperature difference between the environments in thermal contact with the plates ($\theta_2$).

In tables 4 e 5 it is compared, for non-Newtonian fluids with power law indexes equal to 0.25; 1 and 4 , $\theta_2=0$, and a Biot number specified on the upper plate ($Bi_2$), the values of the Local Nusselt numbers on the upper and lower plates. It is possible to verify different values among them, as a result of the condition of asymmetry. It can also be seen that as the Biot number increases, the difference between $Nu_1(X)$ and $Nu_2(X)$ decreases, tending asymptotically the symmetry situation. The same behavior can be verified in Tables 6 and 7.

**Table 4. Comparison of Local Nusselt numbers on the lower and upper plates for $Bi_2$ = 15 and $\theta_2$=0.**

| $X$ / $n$ | $X=0.001$ | | $X=0.01$ | | $X=0.1$ | | $X=1$ | |
|---|---|---|---|---|---|---|---|---|
| | $Nu_1(X)$ | $Nu_2(X)$ | $Nu_1(X)$ | $Nu_2(X)$ | $Nu_1(X)$ | $Nu_2(X)$ | $Nu_1(X)$ | $Nu_2(X)$ |
| *n = 0.25* | 23.6313 | 27.4204 | 11.2416 | 13.0358 | 7.7762 | 9.6056 | 7.73135 | 9.66144 |
| *n = 1.00* | 19.5778 | 22.1299 | 9.7347 | 10.8757 | 7.0764 | 8.3041 | 7.0475 | 8.3390 |
| *n = 4.00* | 18.0403 | 20.2030 | 9.09889 | 10.0359 | 6.74109 | 7.74274 | 6.72069 | 7.76665 |

**Table 5. Comparison of Local Nusselt numbers on the lower and upper plates for $Bi_2$ = 45 and $\theta_2$=0.**

| $X$ / $n$ | $X=0.001$ | | $X=0.01$ | | $X=0.1$ | | $X=1$ | |
|---|---|---|---|---|---|---|---|---|
| | $Nu_1(X)$ | $Nu_2(X)$ | $Nu_1(X)$ | $Nu_2(X)$ | $Nu_1(X)$ | $Nu_2(X)$ | $Nu_1(X)$ | $Nu_2(X)$ |
| *n = 0.25* | 23.7444 | 26.6150 | 11.4353 | 12.1410 | 8.19127 | 8.81987 | 8.17603 | 8.82902 |
| *n = 1.00* | 19.6503 | 20.8582 | 9.8617 | 10.3032 | 7.36641 | 7.79058 | 7.35632 | 7.79736 |
| *n = 4.00* | 18.0998 | 19.1051 | 9.20357 | 9.56354 | 6.98129 | 7.32768 | 6.97408 | 7.33238 |

In tables 6 and 7 it is compared the values of the local Nusselt number in the lower and upper plates for non-Newtonian fluids with power law indexes equal to 0.25; 1 and 4, $\theta_2= 0.1$, and a Biot number in the upper plate ($Bi_2$) specified. A difference of results can be verified in relation to the cases presented in tables 4 and 5, where convergence is established for the local Nusselt number around the value 4, according to increases of $Bi_2$.

**Table 6. Comparison of Local Nusselt numbers on the lower and upper plates for $Bi_2$ = 15 and $\theta_2$=0.1**

| $X$ / $n$ | $X=0.001$ | | $X=0.01$ | | $X=0.1$ | | $X=1$ | |
|---|---|---|---|---|---|---|---|---|
| | $Nu_1(X)$ | $Nu_2(X)$ | $Nu_1(X)$ | $Nu_2(X)$ | $Nu_1(X)$ | $Nu_2(X)$ | $Nu_1(X)$ | $Nu_2(X)$ |
| *n = 0.25* | 23.6112 | 27.5267 | 11.17443 | 13.22375 | 7.41094 | 10.55953 | 4.03685 | 3.95696 |
| *n = 1.00* | 19.5628 | 22.1933 | 9.68377 | 10.9995 | 6.80177 | 8.93678 | 4.06333 | 3.92673 |
| *n = 4.00* | 18.0270 | 20.2540 | 9.05403 | 10.1390 | 6.50394 | 8.26068 | 4.07948 | 3.90776 |

**Table 7. Comparison of Local Nusselt numbers on the lower and upper plates for $Bi_2$ = 45 and $\theta_2$=0.1**

| $X$ / $n$ | $X=0.001$ | | $X=0.01$ | | $X=0.1$ | | $X=1$ | |
|---|---|---|---|---|---|---|---|---|
| | $Nu_1(X)$ | $Nu_2(X)$ | $Nu_1(X)$ | $Nu_2(X)$ | $Nu_1(X)$ | $Nu_2(X)$ | $Nu_1(X)$ | $Nu_2(X)$ |
| *n = 0.25* | 23.7127 | 25.6819 | 11.3464 | 12.2814 | 7.73438 | 9.58221 | 4.02173 | 3.97688 |
| *n = 1.00* | 19.6279 | 20.9007 | 9.79673 | 10.4002 | 7.03278 | 8.31354 | 4.04128 | 3.95598 |
| *n = 4.00* | 18.0805 | 19.1402 | 9.14721 | 9.64579 | 6.69694 | 7.76184 | 4.05414 | 3.94188 |

### 3.2.1 Influence of the power law index (*n*)

At this point, the scope returns to the influence of the power law index on the development of the temperature field. Four distinct power law indexes ($n$=0.25, $n$=1, $n$=4 and $n$=16) are used, respectively representing pseudoplastic, Newtonian and dilatant fluids. For $Bi_2$=10 and $\theta_2$=0.1, we investigate the influence of the fluid rheology on the evolution of the thermal field. The results are shown in Figures 5-10.

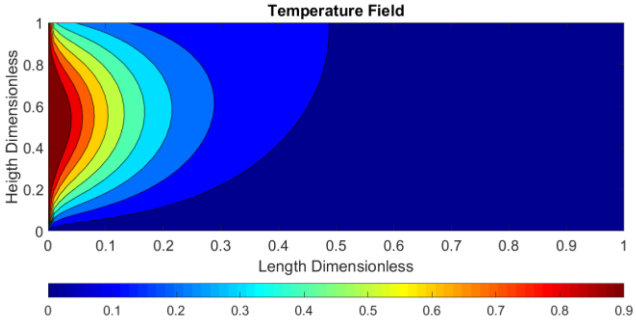


**Figure 5.** Thermal field for $n$=0.25, $Bi_2 = 10$ and $\theta_2=0.1$

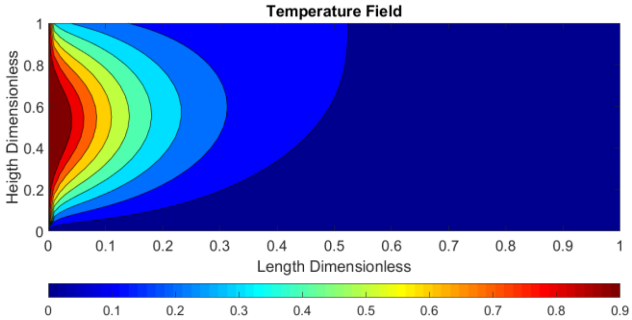


**Figure 6.** Thermal field for $n$=1, $Bi_2 = 10$ and $\theta_2=0.1$

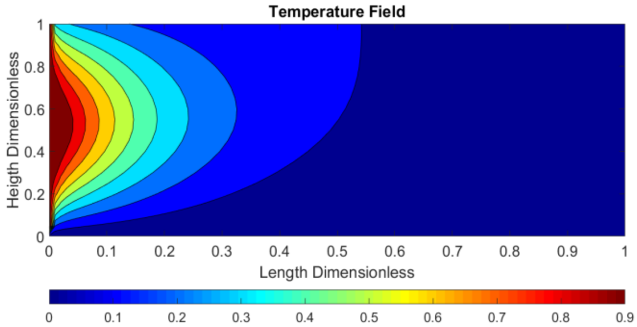


**Figure 7.** Thermal field for $n$=4, $Bi_2 = 10$ and $\theta_2=0.1$

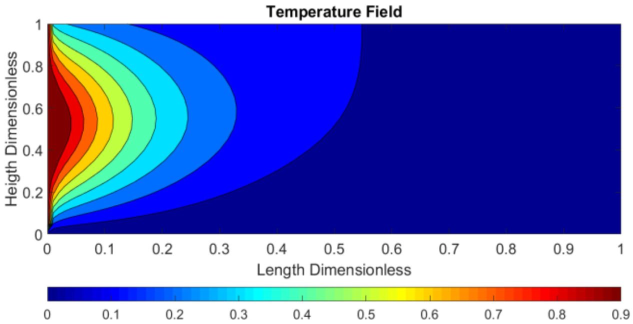


**Figure 8.** Thermal field for $n$=16, $Bi_2 = 10$ and $\theta_2=0.1$

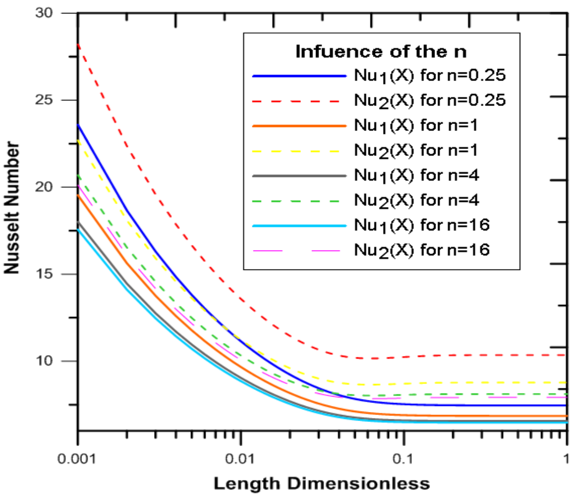


**Figure 9.** Nusselt number for $Bi_2 = 10$ and $\theta_2=0$

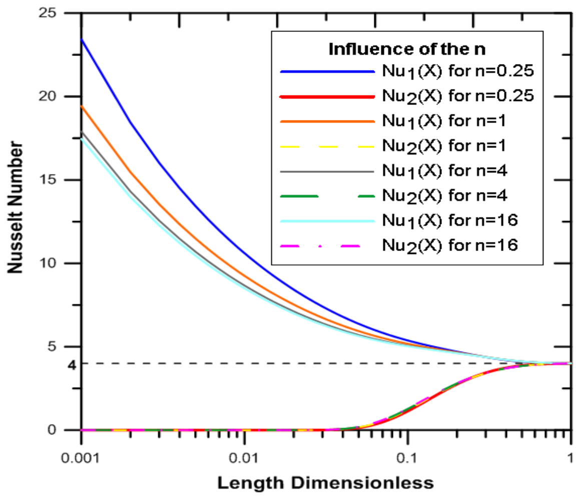


**Figure 10.** Nusselt number for $Bi_2 = 10$ and $\theta_2=1$

The figures 5-10 show that the results are different when different power law indices are considered. Through Figure 9 it can be seen that the Nusselt number converges to smaller values in the proportion in which the power law index increases, and this happens for the nusselt in the lower and upper plate. Also in this figure it can be seen that the Nusselt number converges asymptotically to a common curve, as n increases. In figure 10, due to the temperature difference between the lower and upper plates, it is possible to conclude that there is no convection in the upper plate until a certain dimensionless length from which the Nusselt number ($Nu_2$) begins to increase, converging to the value 4 independent of n.

### 3.2.2 Influence of Biot number on upper plate ($Bi_2$)

In this topic the influence of the Biot number on the upper plate over the temperature field will be discussed. For $n=1$ and $\theta_2=0.3$, the development of the thermal field is evaluated for cases where $Bi_2$ assumes the values 1,10,100 and 1000, respectively. The results are shown in Figures 11-14.

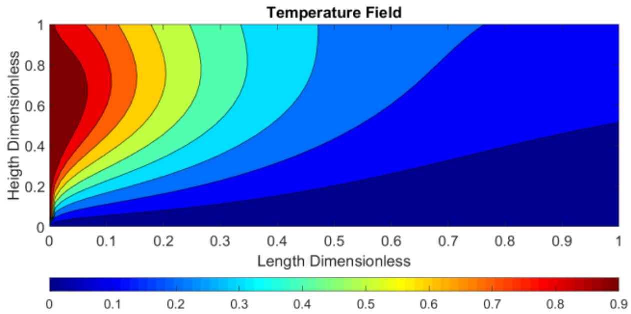


**Figure 11.** Thermal field for $Bi_2$ = *1*, *n=1* and $\theta_2$=*0.3*

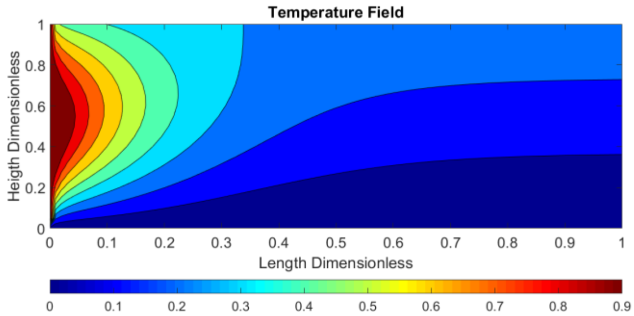


**Figure 12.** Thermal field for $Bi_2$ = *10*, *n=1* and $\theta_2$=*0.3*

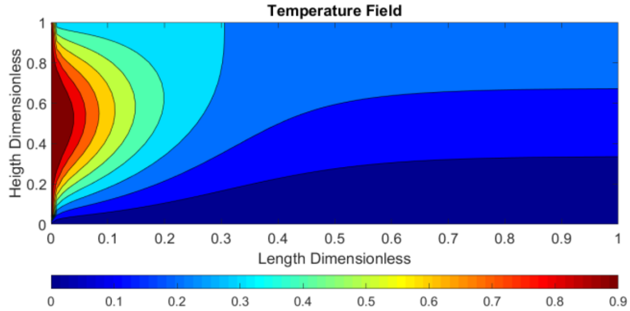


**Figure 13.** Thermal field for $Bi_2$ = *100*, *n=1* and $\theta_2$=*0.3*

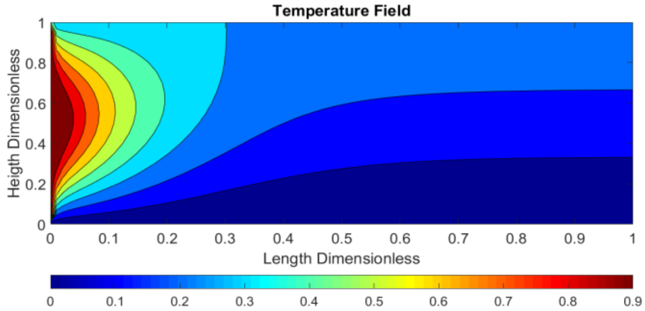


**Figure 14.** Thermal field for $Bi_2$ = *1000*, *n=1* and $\theta_2$=*0.3*

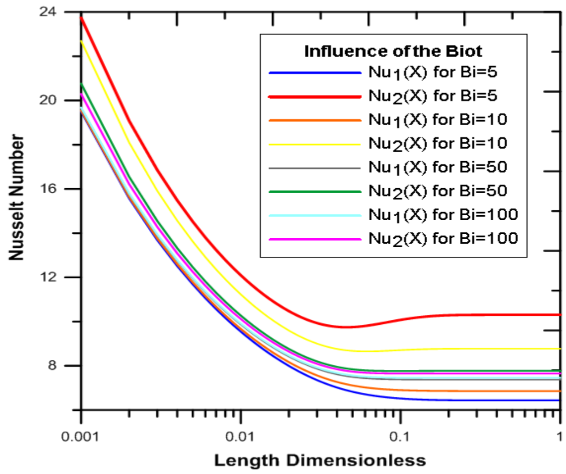


**Figure 15.** Nusselt number for *n* = *1* and $\theta_2$=*0*

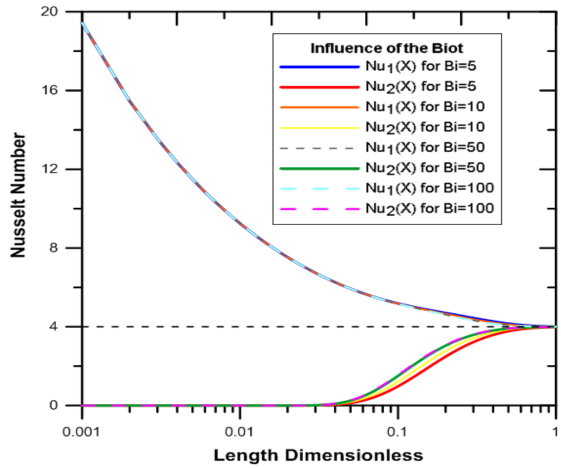


**Figure 16.** Nusselt number for *n*= *1* and $\theta_2$=*1*

In the figures 15 and 16 is possible to observe the influence of the Biot number on the upper plate about the nusselt numbers. Figure 15 shows that the difference between $Nu_1$ (X) and $Nu_2$ (X) decreases as the number of Biot increases, tending asymptotically the situation of symmetry, since we consider $Bi_1 \rightarrow \infty$.

### 3.2.3 Influence of the $\theta_2$

The temperature field is then evaluated for the case where *n*= *1*, $Bi_2 \rightarrow \infty$ e $\theta_2$ assumes the values 0.4, 0.6, 0.8 and 1.0, respectively. It can be seen from Figures 17-20 that the temperature field tends to develop to establish a uniform gradient in the direction of the dimensionless height.

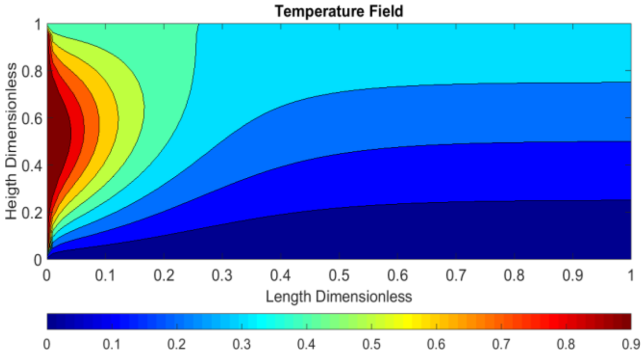


**Figure 17.** Thermal field for $\theta_2$= *0.4*, *n=1* and $Bi_2 \rightarrow \infty$

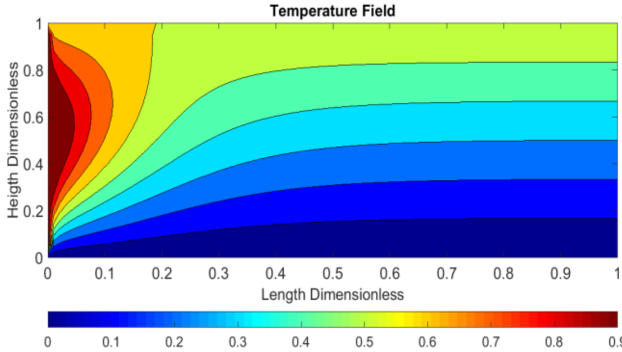


**Figure 18.** Thermal field for $\theta_2$= *0.6*, *n=1* and $Bi_2 \rightarrow \infty$

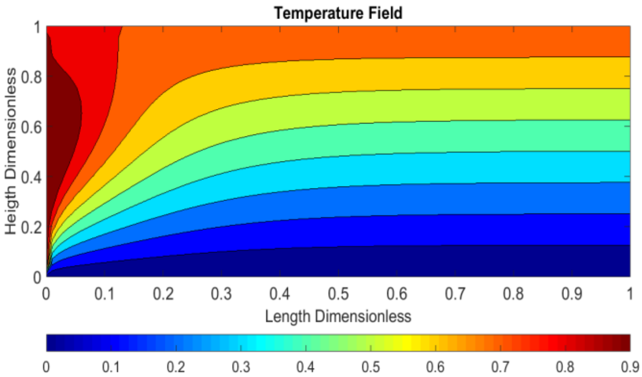


**Figure 19.** Thermal field for $\theta_2 = 0.8$, $n=1$ and $Bi_2 \to \infty$

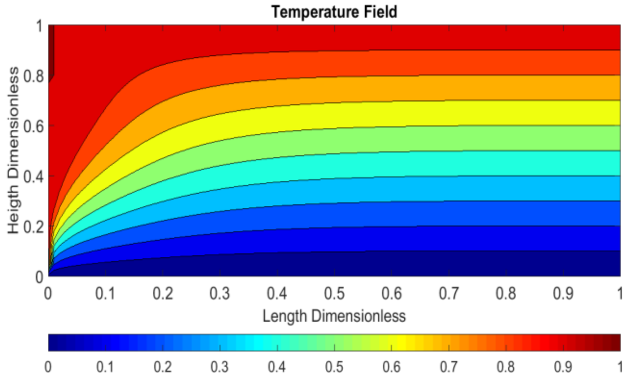


**Figure 20.** Thermal field for $\theta_2 = 1.0$, $n=1$ and $Bi_2 \to \infty$

## 4. CONCLUSIONS

It is concluded, from the analysis of the results obtained, that the application of CITT is effective in solving the problem proposed, since, for the symmetrical case, the presented formulation was validated with the results found in the specialized literature. In this way, the objectives were satisfactorily achieved, where the influence of the power law index and the Biot number on the development of the thermal field and on the local Nusselt numbers in the upper and lower plates was shown. The study carried out in the present work is of great relevance, since it aims to provide parameters for better dimensioning of thermal equipment, as well as providing them with an energy optimization in the process of heat transfer.

## 5. REFERENCES

ASSAD, G.E.; LIMA, J.A.; SANTOS, C.A.C.; LIMA, F.A.; VELOSO, D.L.A.; GONÇALVES, P.G., 2018. "Análise da convecção forçada laminar de fluidos não-newtonianos em dutos retangulares". X Congresso Nacional de Engenharia Mecânica- CONEM 2018.

CHALHUB, D. J. N. M., 2011. "Desenvolvimento de Soluções para Problemas da Advecção-Difusão Combinando Transformação Integral e Métodos Discretos". Dissertação de Mestrado. Escola de Engenharia, UFF. Niterói, Rio de Janeiro.

COTTA, R.M.,1993. "Integral Transform in Computational Heat and Fluid Flow". CRC Press, Boca Raton.

COTTA, R.M., 1998. "The Integral Transform Method in Thermal and Fluid". Science and Engineering, Begell House Inc, NY, USA.

DINIZ, L. S., 2005. "Estudo das Tensões Térmicas no Acoplamento Condução-Radiação em Materiais Semitransparentes"; Tese de doutorado, - CT/UFPB

JOHNSTON, P. R., 1994. "A solution method for the Graetz problem for non-newtonian fluids with Dirichlet and Newmann boundary conditions", Mathl. Comput. Modelling 19, 1-19

KAKAÇ, S. YENER, Y. W. and PRAMUANJAROENKIJ, A., 2014. "Convective Heat Transfer", CRC Press, 3rd edition, New York

MIKHAILOV, M. D. and ÖZISIK, M. N., 1984. "Unified Analysis and Solutions of Heat and Mass Diffusion", John Wiley, New York

MIKHAILOV, M. D. and VULCHANOV, N. L., 1983. "Computational procedure for Sturn-Liouville problems", Journal of computational Physics, v. 5, 323-336

NORRIS, R. H. and STREID, D. D. , 1940. "Laminar flow heat-transfer coefficient for ducts", Trans. ASME, 62, 525–533.

SANTOS, C.A.C.; QUARESMA, J.N.N. and LIMA, J. A., 2001. "Convective Heat Transfer in Ducts: the Integral Transform Approach", 348 p., E-Papers, ABCM Mechanical Sciences Series, Rio de Janeiro, Brazil

SHAH, R.K., 1975. "Thermal entry length solutions for the circular tube and parallel plates", Proc. Natl. Heat Mass Transfer Conf., 3rd, Indian Inst. Techonol., Bombay, Vol. I, Pap. No. HMT-11-75

SHAH, R.K. and LONDON, A.L., 2014. "Laminar Flow Forced Convection in Ducts: A Source Book for Compact Heat Exchanger Analytical Data", vol. 1, Academic Press

VERONESE, J.P.; SILVA, S.A.; MARTINS, C.R; LUCENA, D.V. and SANTOS, J.C., 2012. "Análise da convecção forçada laminar de um fluido não newtoniano do tipo pseudoplástico via GITT", VII Congresso Norte-Nordeste de Pesquisa e Inovação

## 6. RESPONSIBILITY NOTICE